Rare Metal Materials and Engineering
Volume 53, Issue 10, October 2024
Available online at www.rmme.ac.cn

Science Press

Cite this article as: Zhou Cheng, Jin Lei, Jing Gaoyang, et al. Coarsening Behavior of γ′ Precipitates and Compression Performance of Novel Co-Ni-Al-W Superalloy[J]. Rare Metal Materials and Engineering, 2024, 53(10): 2786-2793. DOI: 10.12442/j.issn.1002-185X.20240244.

ARTICLE

Coarsening Behavior of γ′ Precipitates and Compression Performance of Novel Co-Ni-Al-W Superalloy

Zhou Cheng[1,2], Jin Lei[1,2], Jing Gaoyang[1,2], Yu Boyan[1,2], Zhao Jun[1,2]

[1] Shenyang Research Institute of Foundry Co., Ltd, China Academy of Machinery, Shenyang 110022, China; [2] National Key Laboratory of Advanced Casting Technologies, Shenyang 110022, China

Abstract: The coarsening behavior of γ′ precipitate phase at different temperatures and the compressive performance of novel Co-Ni-Al-W superalloy were investigated. Experiment results show that the evolution of the mean radius and volume fraction of the γ′ phase obeys the classical Lifshitz-Slyozov-Wagner model. The coarsening rate of the γ′ phase exhibits a significant dependence on the aging temperature, which increases from 1.30×10^{-27} m^3/s at 800 °C to 9.56×10^{-27} m^3/s at 900 °C. The activation energy of γ′ phase is mainly influenced by the W diffusion in the γ matrix, presenting as 210 kJ/mol. The prepared Co-Ni-Al-W alloy possesses superb comprehensive properties, particularly the good combination of high γ′ solvus temperature (1221 °C) and low density (8.7 g/cm³). Besides, the compressive yield strength of the Co-Ni-Al-W alloy at ambient and high temperatures are higher than that of other γ′-strengthened Co-based superalloys. The compressive yield strength of the Co-Ni-Al-W alloy at 850 °C is as high as 774 MPa.

Key words: Co-Ni-Al-W superalloy; γ′ phase; coarsening behavior; compressive performance

Co-based superalloys possess excellent thermal corrosion resistance, fatigue resistance, and weldability, which are widely suitable for the manufacture of critical hot-end components of aircraft engines and ground gas turbines[1]. Compared with Ni-based superalloys, the traditional Co-based superalloys rely solely on the solid solution strengthening and carbide strengthening, which are severely restricted in the engineering applications at higher temperatures (>800 °C) due to their lack of γ′ phase strengthening effects. Recently, the γ′-Co_3(Al, W) phase with $L1_2$ structure is found in the Co-Al-W-based superalloys[2]. The γ′ phase is stable at high temperatures and coherent with the γ matrix, exhibiting superior high-temperature mechanical properties, compared with traditional Co-based superalloys. These findings promote the development of novel γ′ phase-strengthened Co-based superalloys.

The melting point of Co-Al-W-based alloys is higher than that of Ni-based alloys by nearly 100 °C, and the dissolution temperature of the γ′-Co_3(Al, W) phase exceeds 1000 °C[3]. Furthermore, adding Ta, Nb, or Ti to Co-Al-W-based alloys can effectively increase the dissolution temperature of the γ′ phase[4–6]. Additionally, the small lattice mismatch in Co-Al-W-based alloys can effectively suppress the coarsening of the γ′ phase, resulting in a significant strengthening effect[7]. However, the γ′+γ dual-phase region in Co-Al-W-based alloys is relatively narrow, which is prone to the precipitation of harmful secondary phases during the alloying process[8–9]. For example, in the Co-9Al-10W alloy, the addition of only 2wt%–4wt% refractory elements, such as Ta, Mo, and Nb, can lead to the precipitation of μ and χ phases in the matrix, reducing the volume fraction of γ′ phase. It was found that adding 25wt%–30wt% Ni could expand the γ′ + γ dual-phase region[10]. Therefore, the Co-Ni-Al-W series alloys designed according to this principle can enhance the stability and volume fraction of the γ′ phase and effectively suppress the precipitation of harmful secondary phases[11].

The novel Co-based superalloy employs γ′ precipitates as its primary coherent strengthening phase. The morphology, size, distribution, and volume fraction of γ′ phase play a crucial role in the strengthening effects, thereby influencing the mechanical properties of the alloys under high-temperature conditions. However, exposure to high-temperature environment may lead to microstructure

Received date: April 25, 2024
Foundation item: Natural Science Foundation of Liaoning Province (2023-MSLH-337)
Corresponding author: Zhou Cheng, Ph. D., Senior Engineer, Shenyang Research Institute of Foundry Co., Ltd, China Academy of Machinery, Shenyang 110022, P. R. China, Tel: 0086-24-25851306, E-mail: zhoucheng@chinasrif.com

transformation in the alloy. Therefore, the microstructure stability of the alloy under high-temperature conditions should be optimized to enhance the mechanical properties. Coarsening phenomenon of γ' phase usually serves as a critical factor influencing the microstructure stability and high-temperature mechanical properties. During high-temperature operation, the γ' phase undergoes coarsening and growth processes. The faster the coarsening rate, the more significant the increase in the size of γ' phase, leading to the reduction in the strengthening effect[12–13]. Although the coarsening kinetics of the γ' phase in Ni-based alloys have been studied, the coarsening behavior of Co-based superalloys is rarely reported, particularly for the novel γ' phase-strengthened Co-Ni-Al-W-based alloys[14–15].

In this research, the microstructure evolution of Co-Ni-Al-W-based superalloys after aging under different conditions was investigated. The evolution in the morphology, size, and volume fraction of the γ' phase was studied as a function of the aging process, exploring the influence factors of γ' phase coarsening. The microstructure stability of the Co-Ni-Al-W-based superalloy at high temperatures was discussed. Furthermore, the compressive properties of the Co-Ni-Al-W-based superalloys at 25–950 °C were studied.

1 Experiment

The experiment alloy was melted into ingots using the vacuum induction technique at 1480 °C under the vacuum atmosphere of 0.5 Pa. The cylindrical samples with height of 80 mm and diameter of 15 mm were cast. The composition of the experiment alloy was 41.7Co-27.2Ni-9.0W-6.6Cr-5.7Ta-4.4Ti-3.0Al-2.3Mo-0.02C (wt%), namely Co-Ni-Al-W alloy. The samples were put into quartz tubes filled with pure argon gas to prevent oxidation in the following heat treatment. The heat treatment process included solid solution treatment and aging treatment. The samples were firstly subjected to solid solution treatment at 1230 °C for 24 h and then cooled to room temperature in air. After that, the solid solution-treated samples were aged at 800, 850, and 900 °C for 24, 72, 144, and 216 h and then cooled to room temperature in air.

The morphology, size, and distribution of the γ' phase in the Co-Ni-Al-W alloy were characterized using Ultra-55 field emission scanning electron microscope (SEM). The samples were mechanically ground and polished before electrochemical etching using the mixed solution of 42vol% H_3PO_4+34vol% H_2SO_4+24vol% H_2O. The radius of the γ' precipitate (r) was estimated to be $a/2$, where a represents the mean edge length of the cubic precipitates. SEM images were analyzed using Image-Pro Plus software to calculate the volume fraction of γ' precipitates by measuring their total area.

The phase transformation temperatures of the Co-Ni-Al-W alloys were accurately determined by NETZSCH 404 F3 differential scanning calorimetry (DSC) equipment at the heating rate of 10 °C/min. The mass density measurements were conducted according to ASTM B311-08. Cylindrical samples with 10 mm in diameter and 12 mm in height were prepared for compression tests (Gleeble 3800 thermo-simulator system) at ambient and high temperatures (600–950 °C) under strain rate of 10^{-4} s^{-1}.

2 Results and Discussion

2.1 Microstructure evolution during aging

Fig. 1–Fig. 3 display the size, distribution, and morphology of the γ' phase in Co-Ni-Al-W alloys after aging at 800, 850, and 900 °C for different durations, respectively. The γ' phase is precipitated uniformly in the γ matrix after aging at 800 °C for 24 h and it is spherical with average radius of 52.4 nm, as shown in Fig. 1a. The γ' phase size increases to 76.5 nm after aging for 72 h, as shown in Fig. 1b. After aging for 144 and

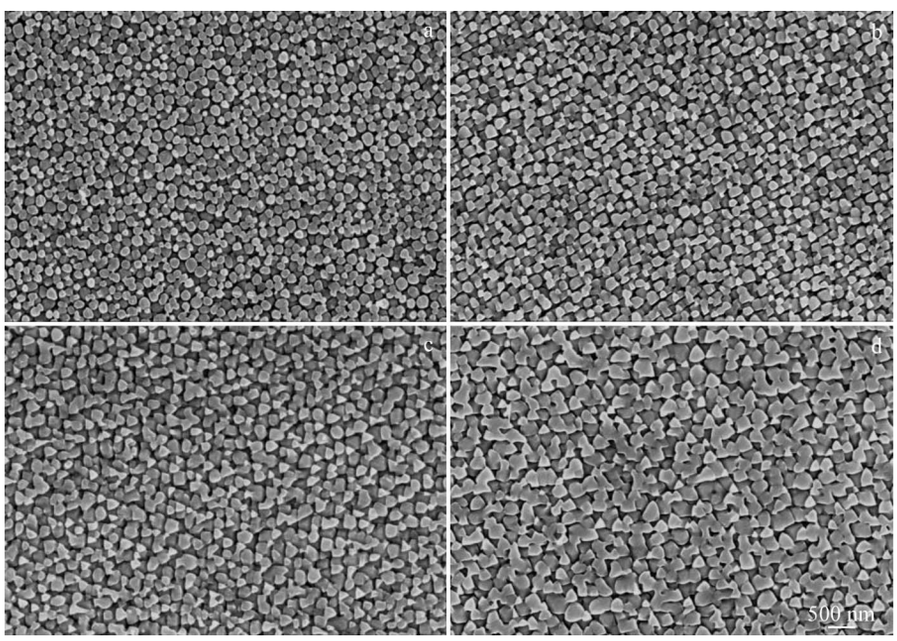

Fig.1 SEM microstructures of Co-Ni-Al-W alloys after aging at 800 °C for 24 h (a), 72 h (b), 144 h (c), and 216 h (d)

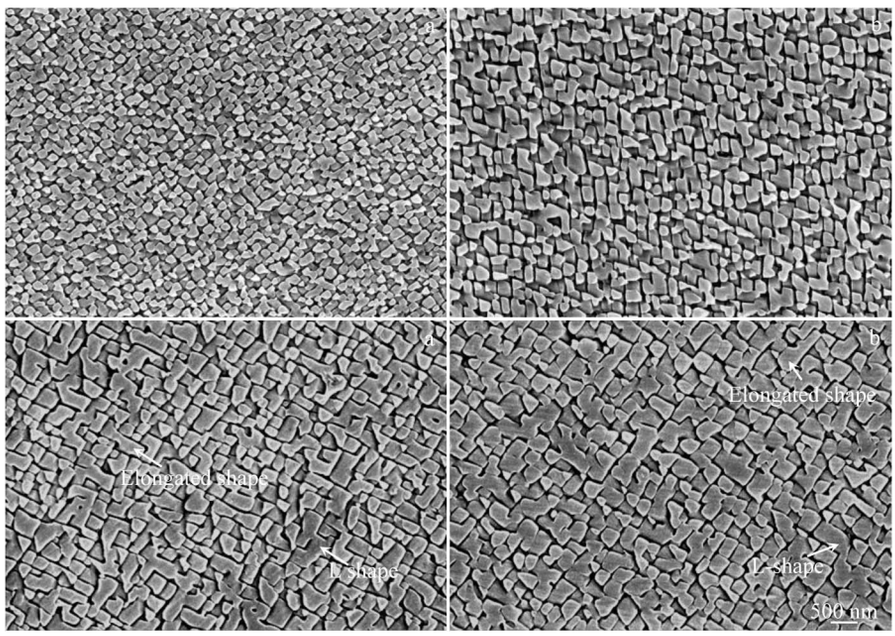

Fig.2 SEM microstructures of Co-Ni-Al-W alloys after aging at 850 °C for 24 h (a), 72 h (b), 144 h (c), and 216 h (d)

216 h, the γ' phase size increases to 91.5 and 103.2 nm, respectively, and some γ' phases change from spherical shape to approximately cubic shape, as shown in Fig. 1c and 1d. Ref. [16 – 18] reported that the morphology of γ' phase was mainly determined by the competition results of the elastic strain energy mechanism and interface energy mechanism of γ/γ' dual-phase. When the elastic strain energy is small and the interface energy dominates, the morphology of γ' phase tends to be spherical. In contrast, the dominance of elastic strain energy will lead to the cubic morphology of γ' phase. After aging at 800 °C for 24 h, the γ' phase size is small, resulting in negligible differences in lattice parameters between the γ' phase and the γ matrix. Hence, there is no significant interaction between the elastic strain energy domains. Therefore, the morphology of the γ' phase is predominantly influenced by the interface energy, resulting in the spherical shape. However, with the prolongation of aging time, the coarsening process of γ' phase generates a mismatch parameter between the γ/γ' dual-phase, leading to the dominance of elastic strain energy. As a result, the spherical γ' phase is prone to the transformation into cubic γ' phase.

Fig.2 shows the microstructures of Co-Ni-Al-W alloys after aging at 850 °C for different durations. It can be seen that the γ' phase primarily exhibits a cubic morphology. With the

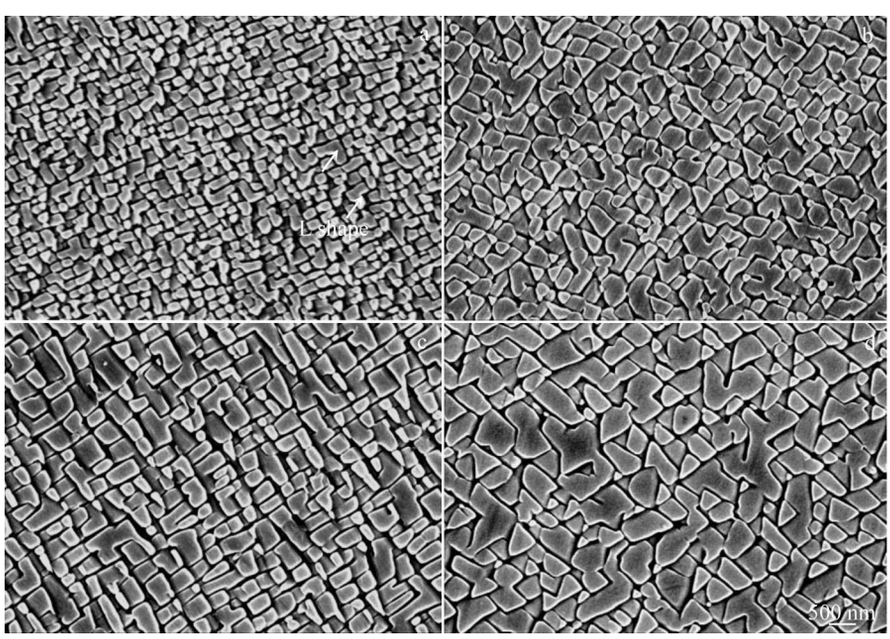

Fig.3 SEM microstructures of Co-Ni-Al-W alloys after aging at 900 °C for 24 h (a), 72 h (b), 144 h (c), and 216 h (d)

prolongation of aging time from 24 h to 216 h, the average size of γ' phase is increased from 70.5 nm to 138.5 nm. Notably, when the aging time exceeds 144 h, the morphology of some γ' phases begins to transform into elongated and L shapes, as indicated by the arrows in Fig. 2c and 2d. The γ' phase in the Co-Ni-Al-W alloy tends to merge along particular directions after aging at 850 °C, which is associated with the atomic arrangement of neighboring γ' phases. When the atomic arrangement of adjacent γ' phases allows for the continuation and expansion of the ordered structure without disruption, the γ' phases are more inclined to merge, thereby reducing surface energy.

When the aging temperature further increases to 900 °C, the γ' phase basically presents the cubic morphology, as shown in Fig.3. With the prolongation of aging time from 24 h to 216 h, the γ' phase becomes larger. The average size of the cubic γ' phase also increases from 100.2 nm to 197.5 nm. Additionally, the elongated- and L-shaped γ' phases are already generated after aging at 900 °C for 24 h (Fig. 3a), indicating that the γ' phase is more prone to coalescence during high-temperature aging. With the further prolongation of aging time to 216 h, more γ' phases merge, resulting in more irregular morphologies (Fig.3d).

Fig. 4 illustrates the evolution of the average size and volume fraction of γ' phase in the Co-Ni-Al-W alloys after different aging treatments. According to Fig. 4a, the average size of the γ' phase increases continuously with aging time under the same aging temperature condition. Additionally, the growth rate of the γ' phase is faster at higher aging temperatures, indicating that the aging temperature controls the growth rate of γ' phase. The volume fractions of γ' phase in the Co-Ni-Al-W alloys aged at 800, 850, and 900 °C for 24 h are 69%, 64%, and 59%, respectively. When the aging time increases to 216 h, the volume fractions of the γ' phase after aging at 800, 850, and 900 °C increases to 73%, 68%, and 65%, respectively, as shown in Fig.4b.

Therefore, it is concluded that the volume fraction of γ' phase is slightly increased with the prolongation of aging time under the same aging temperature. This phenomenon is primarily attributed to the growth of γ' phase during the continuous aging process, thereby increasing the γ' phase volume fraction. However, the increase in the aging temperature results in a decrease in the precipitation of γ' phase, which in turn decreases the volume fraction of the γ' phase. Additionally, the merging of γ' phases, namely the formation of large phases through the consumption of small phases, ultimately results in the decrease in the volume fraction of the γ' phase[19]. On the other hand, aging at lower temperatures leads to the higher volume fraction of precipitated γ' phase, which is caused by the higher solute supersaturation rather than the aging at 900 °C.

2.2 Coarsening behavior of γ' phase during aging

Ref. [20 – 22] suggested that the γ' phase in Ni-based superalloys coarsens via Ostwald ripening, which can be well-explained by the diffusion-controlled coarsening theory proposed by Lifshitz, Slyozov[20], and Wagner, namely the Lifshitz-Slyozov-Wagner (LSW) coarsening model. LSW model explains a competitive growth mechanism in particle growth, where large particles merge small particles. The driving force for growth lies in the reduction of interfacial energy of the system, and the coarsening rate depends on the diffusion of solute elements in the γ matrix. Additionally, Ardell and Ozolins proposed a trans-interface diffusion-controlled (TIDC) mode, which indicated that the diffusion of solute elements through the γ/γ' interface controlled the coarsening process[23–24]. Eq. (1) can aptly describe the correlation between the aging time and the size of γ' phase, as follows:

$$r_t^n - r_0^n = K(t - t_0) \quad (1)$$

where r_t is the radius of γ' phase aged for t h; r_0 is the radius of γ' phase aged for t_0 h; n is the time exponent; K is the coarsening rate coefficient. The controlling mechanism of the coarsening rate in two models mainly depends on the time exponent n in Eq.(1). The time exponent n in LSW model is 3, whereas that in TIDC model is 2.

To clarify the coarsening kinetics of γ' phase in the Co-Ni-Al-W alloy, it is necessary to determine the value of time exponent n in Eq.(1). Fig.5 shows the logarithmic relationship between the average radius of γ' phase and aging time. The slope based on the linear fitting analysis represents the reciprocal relationship of the time exponent as $1/n$. According to Table 1, the slopes after aging at 800, 850, and 900 °C for

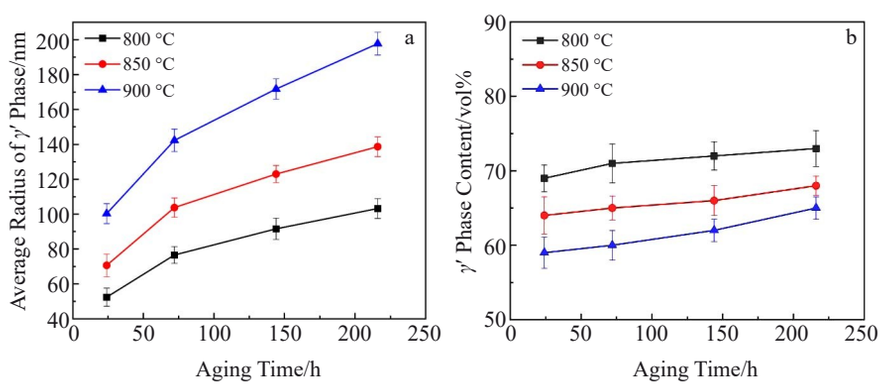

Fig.4 Evolution of average radius (a) and content (b) of γ' precipitate phases after different aging treatments

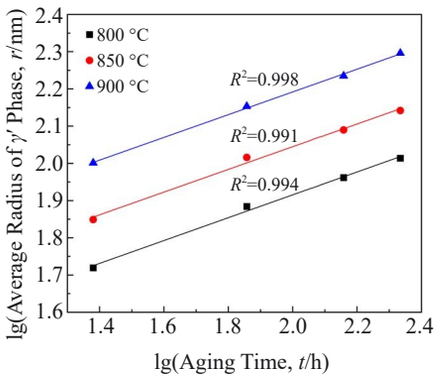

Fig.5 Relationship of lg*r*-lg*t* of γ' phase under different aging conditions

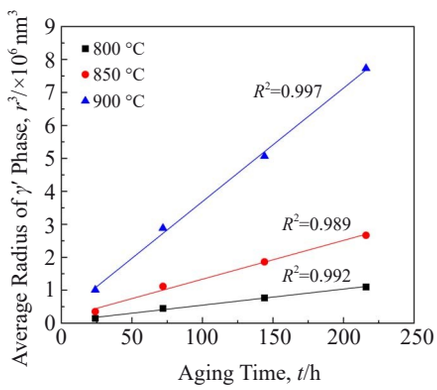

Fig.6 Relationship of r^3-t of γ' phase under different aging conditions

Table 1 Time exponent n and coarsening rate coefficient K obtained based on linear fitting under different aging conditions

Temperature/ °C	Temporal exponent, 1/n	Coarsening rate coefficient, K/×10^{-27} m^3·s^{-1}
800	0.31	1.30
850	0.30	3.27
900	0.31	9.56

the Co-Ni-Al-W alloy are 0.31, 0.30, and 0.31, respectively, signifying that the time exponent n is 3. Furthermore, the linear fitting analysis of Fig. 5 reveals that R^2 is a statistical measure of the proximity between the measured data and the fitting line. The closer the R^2 value to 1, the stronger the relationship between the independent variable and the dependent variable, and the better the fitting between the fitted line and the measured data. Therefore, the time exponent fits the LSW model theory, indicating that the coarsening of the γ' phase in Co-Ni-Al-W alloy obeys LSW theory. By substituting the time exponent n of 3 into Eq. (1), the cubic relationship between the average radius of the γ' phase (r^3) and aging time (t) can be expressed by Eq.(2), as follows:

$$r_t^3 - r_0^3 = K\left(t - t_0\right) \tag{2}$$

The relationship between the average radius of γ' phase (r^3) and aging time (t) is illustrated in Fig. 6. The coarsening rate coefficient K of γ' phase is determined through the slope based on linear fitting results, as shown in Table 1. After aging treatments at 800, 850, and 900 °C, the value of K of γ' phase for the Co-Ni-Al-W alloy is 1.30×10^{-27}, 3.27×10^{-27}, and 9.56×10^{-27} m^3/s, respectively. The diffusion coefficient of solute atoms is higher at higher aging temperatures, promoting the growth of γ' phase. Therefore, with the increase in aging temperature, the coarsening rate of γ' phase also exhibits a significant upward trend. These results show that the coarsening rate of γ' phase is mainly influenced by aging temperature. Moreover, increasing the aging temperature enhances the coarsening rate of γ' phase. Furthermore, the coarsening of γ' phase in the Co-Ni-Al-W alloy conforms to LSW model, suggesting that the diffusion of solute elements regulates the coarsening process of γ' phase.

In LSW model, the coarsening rate of γ' phase is influenced by various factors, including the diffusion coefficient of solute elements, the interfacial energy between γ and γ' phases, and aging temperature. The coarsening rate coefficient can be expressed by Eq.(3), as follows:

$$K = \frac{\Gamma V_m^2 D C_m}{RT} \tag{3}$$

where D is the diffusion coefficient of the solute element, Γ is the γ/γ' interfacial energy, V_m is the molar volume of the γ' phase, C_m is the equilibrium solubility of solute element, R is the gas constant, and T is the absolute temperature. According to the Arrhenius equation[25], the diffusion coefficient D of solute elements can be represented by Eq.(4), as follows:

$$D = D_0 \exp\left(\frac{-Q}{RT}\right) \tag{4}$$

where D_0 is a constant and Q is the activation energy. Therefore, by combining Eq. (3) and Eq. (4), the relationship between diffusion activation energy and coarsening rate coefficient can be obtained, as expressed by Eq.(5), as follows:

$$\ln\left[K\left(\frac{T}{C_m}\right)\right] = \text{Constant} - \frac{Q}{RT} \tag{5}$$

Assuming that T/C_m is constant in Eq. (5), a linear correlation between ln$K$ and 1/T can be established, as illustrated by the fitting line in Fig. 7. The diffusion activation energy of the solute elements in the Co-Ni-Al-W alloy during aging at 800 – 900 °C is determined as 210 kJ/mol through linear fitting analysis. Notably, compared with the diffusion activation energy of 295 kJ/mol in Ref. [26], the value obtained in this research is relatively lower. In Co-Al-W-based alloys, the coarsening process of γ' phase is mainly influenced by the diffusion of W element in the alloy. Moreover, the diffusion activation energy of the W element in the alloy is increased with the W content[27–28]. Hence, it is inferred that the lower W content in the Co-Ni-Al-W alloy is the main reason for the relatively lower diffusion activation energy.

Furthermore, the grain growth is influenced by temperature gradient, undercooling, and the addition of rare earth elements. Ref. [29–30] reported that adding rare earth oxides, such as CeO_2, can significantly refine the grains. Meanwhile,

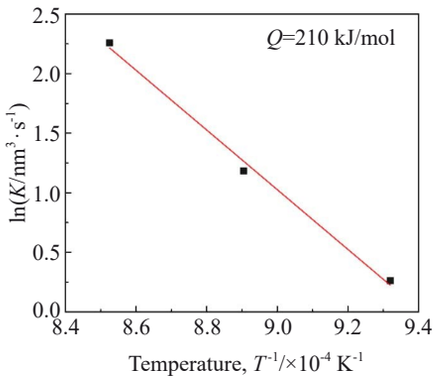

Fig.7 Relationship between ln$K$ and 1/T

the addition of Ti and B elements can achieve a synergistic effect of solid solution strengthening, second phase strengthening, and fine grain strengthening. Therefore, by rationally adding alloying elements, it is possible to regulate the grain size and enhance the mechanical properties.

2.3 Solvus temperature and density comparison

Fig. 8 presents the comparative analysis of solvus temperatures and densities among various Co-based superalloys, including the Co-Ni-Al-W alloy in this research. Notably, the Co-Ni-Al-W alloy stands out with an exceptionally advantageous combination of high solvus temperature (1221 °C) and low density (8.7 g/cm³), surpassing the performance of other alloys. Specifically, the solvus temperature of γ' phase in the Co-Ni-Al-W alloy is significantly elevated, compared with that of other Co-based W-containing superalloys, such as 1000 °C of Co-9Al-9W alloy, 1098 °C of Co-9Al-10W-2Ta alloy[31], and 1166 °C of Co-31Ni-9Al-5W-4Ti-1Ta alloy[32]. Even the Cr-containing alloys, such as Co-Ta-V-based alloys (965 °C) [33], Co-Al-Mo-Ta-based alloys (1038 °C)[34], Co-11Ti-15Cr alloys (1100 °C)[35], and Co-16Ni-10Al-6Cr-5W-3Ta alloy (1100 °C) [36], cannot compete with the Co-Ni-Al-W alloy in the term of solvus temperature.

The Co-Ni-Al-W alloy has a low density of approximately 8.7 g/cm³, as shown in Fig. 8b. This density is notably lower than that of other Co-Al-W-based alloys and commercially available Co-based Mar-M-302 superalloys[37], whose densities are 9.54 – 10.1 and 9.2 g/cm³, respectively. These exceptional characteristics indicate that the Co-Ni-Al-W alloy is a superior alternative to the traditional Co-based alloys, particularly in the lightweight structural applications. Despite its lightweight, the Co-Ni-Al-W alloy maintains its structural integrity and excellent performance, which is ideal for the mass-sensitive applications without compromising the material strength and functionality. These advantageous characteristics position the Co-Ni-Al-W alloy as a promising candidate for high-temperature applications.

2.4 Compressive performance

To investigate the temperature dependence of compressive yield strength of Co-Ni-Al-W alloy, compression tests were conducted at 25–950 °C. The compressive yield strengths of the Co-Ni-Al-W alloy and other Co-based superalloys[31–32,34,36–37] are presented in Fig.9.

The compressive yield strength of the Co-Ni-Al-W alloy can be divided into three stages. In the first stage, the compressive yield strength is decreased with the increase in temperature from 25 °C to 650 °C. In the second stage, the compressive yield strength exhibits a positive temperature dependence when the temperature increases from 650 °C to 850 °C. This phenomenon is similar to that in Ni-based superalloys. Finally, the third stage demonstrates a negative temperature dependence of compressive yield strength above 850 °C. Apart from the first stage, the yield strength decreases from 761 MPa to 714 MPa when the temperature increases from 600 to 650 °C. Subsequently, it gradually increases, reaching a maximum compressive yield strength of 774 MPa at 850 °C. However, with the further increase in temperature to 950 °C, the compressive yield strength decreases to 651 MPa. It is worth noting that the Co-Ni-Al-W alloy exhibits an anomaly behavior in compressive yield strength within the temperature range of 650–850 °C. This behavior can also be

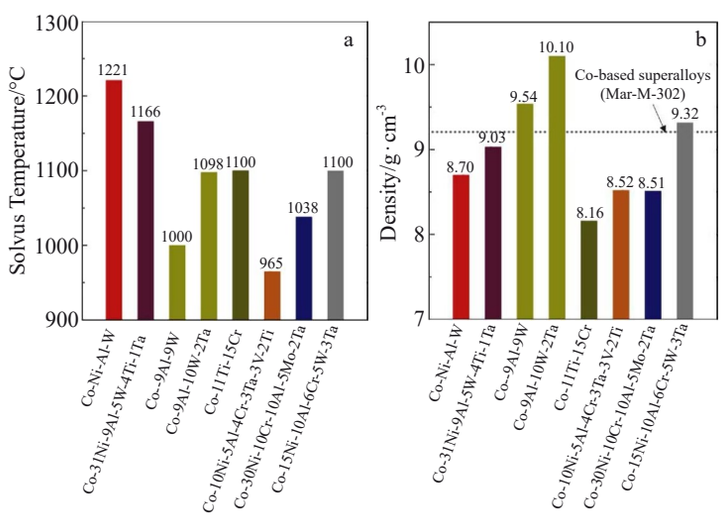

Fig.8 Comparison of solvus temperature (a) and density (b) of Co-Ni-Al-W alloys and Co-based superalloys

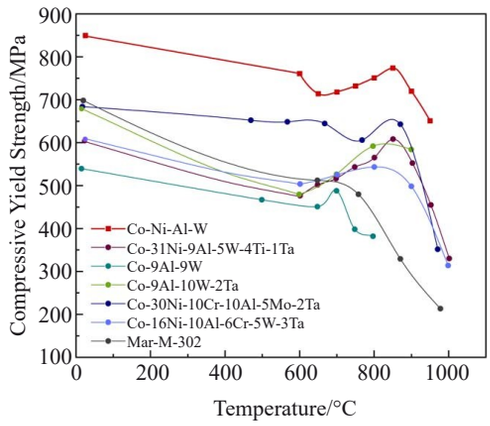

Fig.9 Compressive yield strengths of Co-Ni-Al-W and Co-based superalloys at different temperatures

observed in superalloys contain γ'-strengthened Co-Ti[35,38] and Co-Al-W[31,39], which is associated with the Kear-Wilsdorf mechanism involving the dislocation hindrance at high temperatures[40–42]. Additionally, the Co-Ni-Al-W superalloy has better mechanical properties at high temperatures than other W-free/Cr-containing γ/γ' Co-based superalloys, as shown in Fig.9.

3 Conclusions

1) The microstructure of the Co-Ni-Al-W superalloy aged at 800 °C for 24 h primarily consists of γ matrix phase and 69vol% γ' phase. The Co-Ni-Al-W superalloy has high γ' solvus temperature of 1221 °C and low density of 8.7 g/cm³.

2) The γ' phase morphology changes from spherical to cubic in the Co-Ni-Al-W superalloy aged at 800–900 °C. The average radius grows with higher aging temperatures and longer time. The γ' phase volume fraction is decreased with the increase in temperature but increased with the prolongation of aging time.

3) The coarsening behavior of γ' phase in the Co-Ni-Al-W superalloy obeys the diffusion-controlled LSW coarsening mode. The γ' phase coarsening rate coefficients are 1.30×10^{-27}, 3.27×10^{-27}, and 9.56×10^{-27} m^3/s at 800, 850, and 900 °C, respectively.

4) The activation energy for the Co-Ni-Al-W superalloy is 210 kJ/mol during aging at 800–900 °C, which is related to the W content in the alloy. The diffusion of W element in the alloy affects the coarsening rate of γ' phase.

5) The compressive yield strength curve of the Co-Ni-Al-W alloy has three variation stages. With the increase in temperature from 650 °C to 850 °C, the compressive yield strength exhibits a positive temperature dependence and reaches the maximum compressive yield strength of 774 MPa at 850 °C.

References

1 Feng Qiang, Lu Song, Li Wendao *et al*. *Acta Metallurgica Sinica*[J], 2023, 59(9): 1125 (in Chinese)

2 Sato J, Omori T, Oikawa I *et al*. *Science*[J], 2006, 312(5770): 90

3 Ooshima M, Tanaka K, Okamoto N L *et al*. *Journal of Alloys and Compounds*[J], 2010, 508(1):71

4 Bauer A, Neumeier S, Pyczak F *et al*. *Scripta Materialia*[J], 2010, 63(12): 1197

5 Kobayashi S, Tsukamoto Y, Takasugi T. *Intermetallics*[J], 2012, 31: 94

6 Xu Yangtao, Xia Rongli, Sha Qizhen *et al*. *Rare Metal Materials and Engineering*[J], 2017, 46(9): 2459 (in Chinese)

7 Zhao Y S, Zhang Y H, Zhang Y *et al*. *Progress in Natural Science: Materials International*[J], 2021, 31(5): 641

8 Li Y Z, Florian P, Michael O *et al*. *Journal of Alloys and Compounds*[J], 2017, 729: 266

9 Xu Yangtao, Xia Rongli, Lou Dechao. *Rare Metal Materials and Engineering*[J], 2017, 46(8): 2288 (in Chinese)

10 Omori T, Oikawa K, Sato J *et al*. *Intermetallics*[J], 2013, 32(1): 74

11 Shinagawa K, Omori T, Sato J *et al*. *Materials Transactions*[J], 2008, 49(6): 1474

12 Ges A M, Fornaro O, Palacio H A. *Materials Science and Engineering A*[J], 2007, 458(1): 96

13 Tiley J, Viswanathan G B, Srinivasan R *et al*. *Acta Materialia*[J], 2009, 57(8): 2538

14 Vorontsov V A, Barnard J S, Rahman K M *et al*. *Acta Materialia*[J], 2016, 120(11): 14

15 Sauza D J, Bocchini P J, Dunand D C *et al*. *Acta Materialia*[J], 2016, 117(9): 135

16 Aliakbari-Sani S, Vafaeenezhad H, Arabi H *et al*. *Journal of Materials Research and Technology*[J], 2022, 21: 3425

17 Xu L, Tian C G, Cui C Y *et al*. *Materials Science and Technology*[J], 2014, 30(8): 962

18 Liu Zhaofeng, Cheng Junyi, Ma Xiangdong *et al*. *Rare Metal Materials and Engineering*[J], 2024, 53(3): 768 (in Chinese)

19 Guan Y, Liu Y C, Ma Z Q *et al*. *Vacuum*[J], 2020, 175: 109247

20 Lifshitz I M, Slyozov V V. *Journal of Physics and Chemistry of Solids*[J], 1961, 19(1): 35

21 James C, Hector B, David D. *Acta Materialia*[J], 2010, 58(11): 4019

22 Zhao Guangdi, Zang Ximin, Zhao Zhuo. *Rare Metal Materials and Engineering*[J], 2020, 49(11): 3809 (in Chinese)

23 Alan J A, Vidvuds O. *Nature Materials*[J], 2005, 4(4): 309

24 Long Anping, Xiong Jiangying, Zhang Gaoxiang *et al*. *Rare Metal Materials and Engineering*[J], 2024, 53(4): 1042 (in Chinese)

25 Qu S S, Li Y J, Wang C P *et al*. *Materials Science and Engineering A*[J], 2020, 787: 139455

26 Meher S, Nag S, Tiley J *et al*. *Acta Materialia*[J], 2013, 61(11): 4266

27 Daniel J S, David C D, Ronald D N *et al*. *Acta Materialia*[J], 2019, 164: 654

28 Ravi R, Paul A. *Intermetallics*[J], 2011, 19(3): 426

29 Gao Z T, Ren H B, Geng H M *et al*. *Journal of Materials Engineering and Performance*[J], 2022, 31(11): 9534
30 Gao Z T, Li J Z, Ke L C *et al*. *Journal of Alloys and Compounds*[J], 2023, 966: 171560
31 Suzuki A, DeNolf G C, Pollock T M. *Scripta Materialia*[J], 2007, 56(5): 385
32 Qu S S, Li Y J, He M L *et al*. *Materials Science and Engineering A*[J], 2019, 761: 138034
33 Reyes F L, Taylor S, Dunand D C. *Acta Materialia*[J], 2019, 172: 44
34 Nithin B, Samanta A, Makineni S K *et al*. *Journal of Materials Science*[J], 2017, 52(18): 11036
35 Christopher H Z, Povstugar I, Li R *et al*. *Acta Materialia*[J], 2017, 135: 244
36 Pandey P, Makineni S K, Samanta A *et al*. *Acta Materialia*[J], 2019, 163: 140
37 Makineni S K, Samanta A, Rojhirunsakool T *et al*. *Acta Materialia*[J] 2015, 97(9): 29
38 Ruan J J, Liu X J, Yang S Y *et al*. *Intermetallics*[J], 2018, 92(1): 126
39 Suzuki A, Pollock T M. *Acta Materialia*[J], 2008, 56(6): 1288
40 Caillard D, Molénat G, Paidar V. *Materials Science and Engineering A*[J], 1997, 234(8): 695
41 Wee D M, Noguchi O, Oya, Y *et al*. *Transactions of the Japan Institute of Metals*[J], 1980, 21(4): 237
42 Paidar V, Pope D P, Vitek V. *Acta Materialia*[J], 1984, 32(3): 435

新型Co-Ni-Al-W高温合金γ′析出相粗化行为及压缩性能

周　成[1,2]，金　磊[1,2]，荆高扬[1,2]，于伯岩[1,2]，赵　军[1,2]
(1. 中国机械总院集团 沈阳铸造研究所有限公司，辽宁 沈阳 110022)
(2. 高端装备铸造技术全国重点实验室，辽宁 沈阳 110022)

摘　要：研究了一种新型Co-Ni-Al-W高温合金的γ′析出相在多种温度条件下的粗化行为及合金的压缩性能。实验结果表明，合金在时效过程中，γ′相平均半径和体积分数的演化遵循经典的Lifshitz-Slyozov-Wagner模型。γ′相的粗化速率显著依赖于时效温度，具体表现为从800 ℃时的1.30×10^{-27} m^3/s增加到900 ℃时的9.56×10^{-27} m^3/s。γ′相的活化能主要受W元素在γ基体中的扩散影响，其活化能为210 kJ/mol。所制备的Co-Ni-Al-W合金表现出优异的综合性能，特别是具有高γ′相溶解温度（1221 ℃）和低密度（8.7 g/cm^3）的良好结合。此外，Co-Ni-Al-W合金在常温和高温下的压缩屈服强度均高于其他γ′强化的Co基高温合金，且该合金在850 ℃下的压缩屈服强度高达774 MPa。

关键词：Co-Ni-Al-W高温合金；γ′相；粗化行为；压缩性能

作者简介：周　成，男，1985年生，博士，高级工程师，中国机械总院集团沈阳铸造研究所有限公司，辽宁 沈阳 110022，电话：024-25851306，E-mail：zhoucheng@chinasrif.com